Engineering Fracture Mechanics Vol. 35, No. 1/2/3, pp. 241–250, 1990
Printed in Great Britain.

0013-7944/90 $3.00 + 0.00
Pergamon Press plc.

SNAP-BACK FRACTURE INSTABILITY IN ROCK SPECIMENS: EXPERIMENTAL DETECTION THROUGH A NEGATIVE IMPULSE

PIETRO BOCCA
Istituto Universitario di Architettura di Venezia, 30125 Venice, Italy

and

ALBERTO CARPINTERI
Department of Structural Engineering, Politecnico di Torino, 10129 Torino, Italy

Abstract—Marble specimens were tested in bending to determine the amount of energy recovered in catastrophic (snap-back) failure. Such energy is released in the time period immediately following the achievement of the peak load and it is measured statically in the case of slow and controlled failure modes or dynamically in the case of instantaneous failure modes. An evident increase in recovered energy, W^*, is observed by increasing specimen length, especially if compared with the ultimate elastic energy, W_e, contained in the body at failure.

INTRODUCTION

In some materials, such as rocks and concrete, especially when they possess very high strength, catastrophical (snap-back) failure gives rise to the release of a remarkable amount of energy[1, 2]. In the event of a potentially unstable fracture process, such energy can be measured statically, for instance, by controlling crack mouth opening displacement in specimens tested in bending[3–5]. If failure becomes instantaneous when increasing the brittleness of the specimen, however, the static method will no longer be applicable.

This paper demonstrates that the amount of energy recovered can be measured dynamically[6] through a negative impulse produced by the specimen in the time interval immediately following the achievement of peak load.

The tests were performed on marble specimens in bending. First, the brittleness of the specimen is shown to vary by varying specimen slenderness from a theoretical standpoint; then the amount of energy recovered is measured, statically in the case of less slender specimens, and with a dynamic detector for the slenderer ones undergoing instantaneous failure.

THEORETICAL APPROACH TO THE PROBLEM

Let us consider a specimen with slenderness $\lambda = l/b$, where l = beam span and b = beam depth.

The linear elastic behaviour of a three point bending initially uncracked beam may be represented by the following dimensionless equation:

$$\tilde{P} = \frac{4}{\lambda^3}\tilde{\delta} \tag{1}$$

where the dimensionless load and central deflection are respectively given by:

$$\tilde{P} = \frac{Pl}{\sigma_u t b^2}, \quad \tilde{\delta} = \frac{\delta l}{\epsilon_u b^2}$$

being t = beam thickness, σ_u = ultimate tensile strength, ϵ_u = ultimate tensile strain.

Once the ultimate tensile strength σ_u is achieved at the lower beam edge, a fracturing process in the central cross-section is supposed to start. Such a process admits a limit-situation like that in Fig. 1. The limit stage of the fracturing and deformation process may be considered as that of

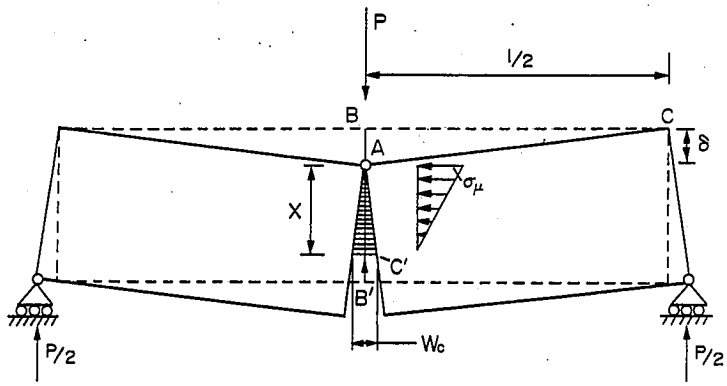

Fig. 1. Limit-situation of complete fracture with cohesive forces.

two rigid parts connected by the hinge A in the upper beam edge. The equilibrium of each part is ensured by the external load, the support reaction and the closing cohesive forces. The last depend on the distance between the two interacting surfaces: increasing the distance w, the cohesive forces decrease linearly until they vanish for $w \geq w_c$.

The geometrical similitude of the triangles ABC and AB′C′ in Fig. 1 provides:

$$\frac{\delta}{l/2} = \frac{w_c/2}{x} \tag{2}$$

where x is the extension of the triangular distribution of cohesive forces. Equation (2) can be rearranged as:

$$x = \frac{w_c l}{4\delta}. \tag{3}$$

The rotational equilibrium round point A is possible for each beam part only if the moments of support reaction and cohesive forces, respectively, are equal:

$$\frac{P}{2}\frac{l}{2} = \frac{\sigma_u x t}{2}\frac{x}{3}. \tag{4}$$

Recalling eq. (3), the relation between load and deflection may be obtained:

$$P = \frac{\sigma_u t l w_c^2}{24}\frac{1}{\delta^2}. \tag{5}$$

Equation (5) can be put into dimensionless form:

$$\tilde{P} = \frac{1}{6}\left(\frac{s_E \lambda^2}{\epsilon_u \tilde{\delta}}\right)^2 \tag{6}$$

where $s_E = w_c/2b$ is the brittleness number of the specimen[1].

While the linear equation (1) describes the elastic behaviour of the beam, initially uncracked, the hyperbolic equation (6) represents the asymptotical behaviour of the same beam, totally cracked. Equation (1) is valid only for load values lower than that producing the ultimate tensile strength σ_u at the lower beam edge:

$$\tilde{P} \leq \tfrac{2}{3}. \tag{7}$$

On the other hand, eq. (6) is valid only for deflection values higher than that producing a cohesive zone of extension x equal to the beam depth b:

$$x \leq b. \tag{8}$$

From eqs (3) and (8) it follows:

$$\tilde{\delta} \geq \frac{s_E \lambda^2}{2\epsilon_u}. \tag{9}$$

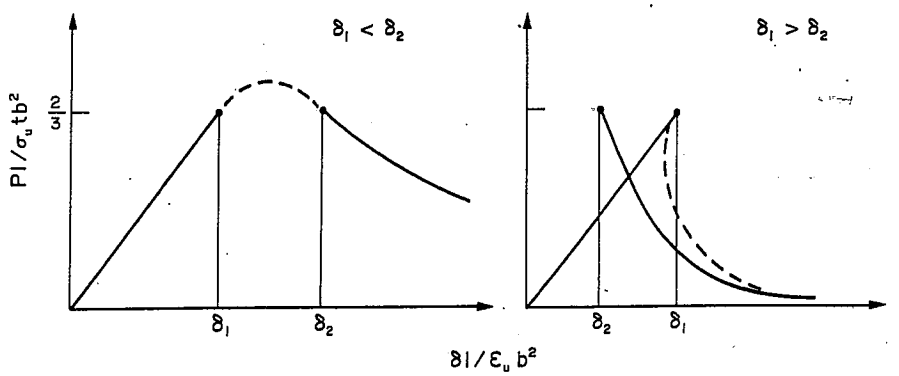

Fig. 2. Load–deflection diagrams: (a) ductile and (b) brittle condition. $\delta_1 = \lambda^3/6$; $\delta_2 = s_E\lambda^2/3\epsilon_u$.

The bounds (7) and (9), upper for load and lower for deflection respectively, can be transformed into two equivalent bounds, both upper for deflection and load. Equations (1) and (7) provide:

$$\tilde{\delta} \leq \frac{\lambda^3}{6} \tag{10}$$

whereas eqs (6) and (9):

$$\tilde{P} \leq \tfrac{2}{3}. \tag{11}$$

Conditions (7) and (11) are coincident. Therefore, a stability criterion for elastic-softening beams may be obtained comparing eqs (9) and (10). When the two domains are separated, it is presumable that the two P–δ branches—linear and hyperbolic—are connected by a regular curve (Fig. 2a). On the other hand, when the two domains are partially overlapped, it is well-founded to suppose them as connected by a curve with highly negative or even positive slope (Fig. 2b).

Unstable behaviour and catastrophical events are then expected for:

$$\frac{s_E\lambda^2}{2\epsilon_u} \leq \frac{\lambda^3}{6} \tag{12}$$

and the brittleness condition for the three point geometry becomes:

$$\frac{s_E}{\epsilon_u\lambda} \leq \tfrac{1}{3}. \tag{13}$$

Thus brittleness increases with increasing slenderness, for the same values of brittleness number s_E and ultimate deformation ϵ_u.

From eq. (13) it can be seen that the structure behaviour shifts from ductile (case D in Fig. 3) to catastrophic (case C in Fig. 3) as the slenderness, λ, is increased.

By analysing the curve in Fig. 4 it appears evident that from point 1 to point 2 we

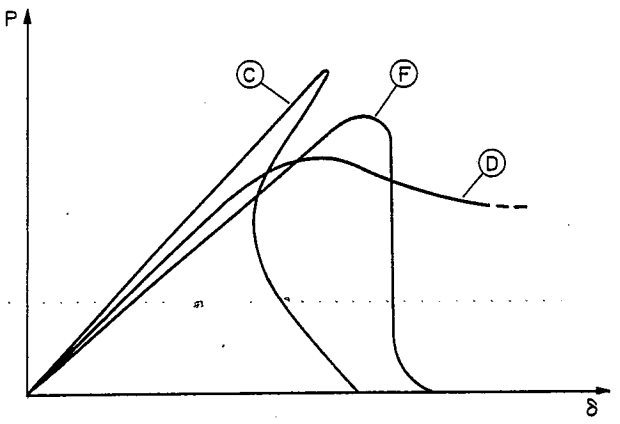

Fig. 3. Load–deflection diagrams corresponding to: D = ductile failure, F = brittle failure, C = catastrophic failure.

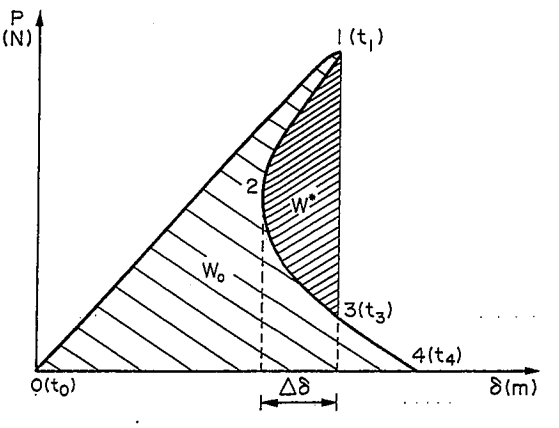

Fig. 4. Load–deflection diagram corresponding to a catastrophic failure. W^* = recovered energy; W_0 = total fracture energy.

get a derivative $dP/d\delta$ with positive sign, corresponding to an inversion in the loading point displacement.

The energy stored in the specimen in the stage $\overline{01}$, W_e, is partially recovered in the stage $\overline{1-2}$ and the area W^*, defined by the boundary $\overline{123}$, therefore represents the total energy recovered by the specimen during failure. The greater the specimen slenderness is, the greater the percentage of energy W^* compared with W_e, results to be on the basis of eq. (13). W^* is determined statically by controlling the crack mouth opening displacement[3, 4, 6, 7, 8].

On the other hand, for high slenderness values involving instantaneous specimen failure, these methods prove inadequate. In such cases, W^* can be measured dynamically through a negative impulse of the specimen against the testing machine, in the time interval immediately following the achievement of the peak load.

NEGATIVE IMPULSE METHOD

The negative impulse method can be briefly summarized as follows.

(1) Measure of the impulse transmitted by the specimen to the testing machine at failure in the time interval t_1–t_3 (see Fig. 4).

(2) Analysis of the impulse and of the corresponding momentum.

(3) Calculation of the energy W^* during the failure process.

The following assumptions are also made.

(i) Specimen failure is instantaneous, that is, the time interval between t_1 and t_3 is infinitesimal and equal to dt.

(ii) The variation in the displacement, $d\delta$, of the loading point over the time interval dt, tends to zero and hence can be neglected.

If specimen failure occurs in bending according to Fig. 5, with the rotation of two rigid parts around their centre of instantaneous rotation C, the angular momentum theorem can be applied as follows:

$$\tfrac{1}{2} l \int_{t_1}^{t_3} F \, dt = I_C \cdot \dot{\theta} \tag{14}$$

where I_C is twice the moment of inertia of the single part valuated with respect to the centre C and can be written as:

$$I_C = I_G + m \cdot \overline{CG}^2 \tag{15}$$

I_G being the baricentric moment of inertia, m the specimen mass, $\overline{CG}$ the distance between point C (centre of instantaneous rotation) and the barycentre of the single part, $\dot{\theta}$ the angular velocity. From eq. (14) we deduce:

$$\dot{\theta} = \frac{1}{2 I_C} \int_{t_1}^{t_3} F \, dt. \tag{16}$$

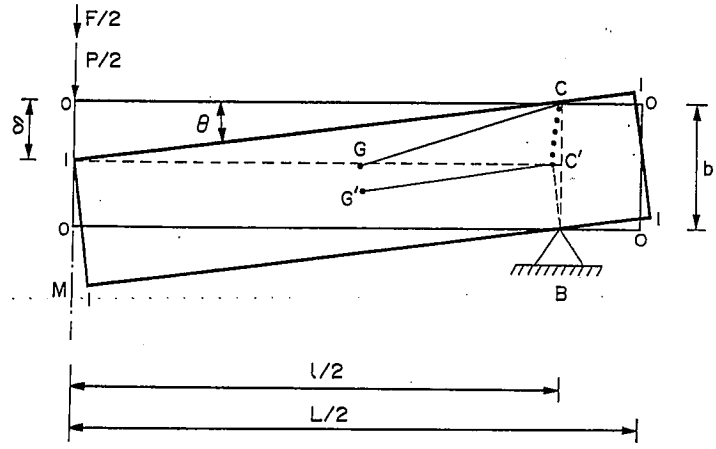

Fig. 5. Kinematics of the fracturing specimen in flexure.

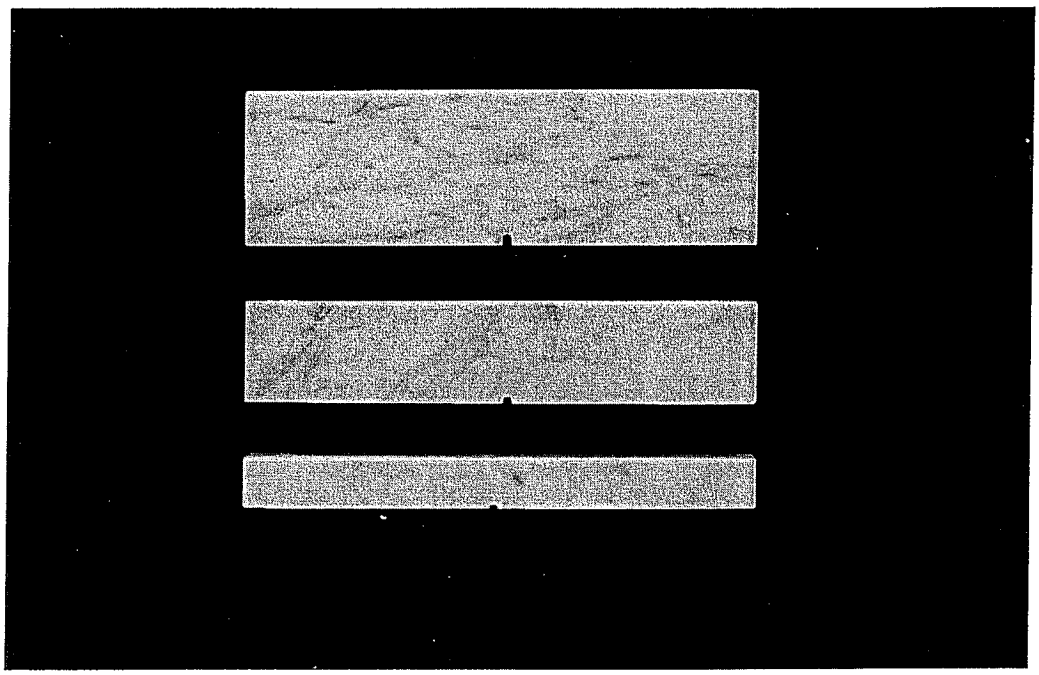

Fig. 6. Specimens with different slenderness.

The variation in kinetic energy associated with the specimen is found to be:

$$T = \tfrac{1}{2} I_C \dot{\theta}^2. \tag{17}$$

The distance $\overline{CG}$ in eq. (15) is obtainable from simple geometrical considerations and it is a function of the displacement δ:

$$\overline{CG} = \sqrt{(\tfrac{1}{2} b/\cos\theta - \tfrac{1}{4} L\theta)^2 + (\tfrac{1}{2} l - \tfrac{1}{4} L - b\theta)^2} \quad \text{if} \quad \delta \neq 0 \tag{18}$$

$$\overline{CG} = \sqrt{(\tfrac{1}{2} b)^2 + (\tfrac{1}{2} l - \tfrac{1}{4} L)^2} \quad \text{if} \quad \delta = 0. \tag{19}$$

Moreover we have:

$$I_G = m \cdot \frac{(L/2)^2 + b^2}{12}. \tag{20}$$

From eqs (16) and (17) we get:

$$T = \frac{\left(\int_{t_1}^{t_3} F \, dt\right)^2 \cdot l^2}{8 I_C}. \tag{21}$$

When friction and dissipative phenomena between specimen and testing machine can be neglected, the theorem of kinetic energy provides:

$$T = W^*. \tag{22}$$

The work W^* (Fig. 4) of all the forces applied to the specimen is therefore equal to the variation in kinetic energy T.

Thus, by measuring the impulse with an impact force transducer placed between specimen and loading machine, the amount of energy W^* can be calculated through eqs (16) to (22).

TESTING PROCEDURE

The tests were carried out on specimens of Carrara marble (Fig. 6) with the characteristics shown in Table 1.

For low slenderness values, $\lambda = l/b (\lambda_1, \lambda_2, \lambda_3)$, the specimens were tested in three point bending, making use of an MTS machine with maximum loading capacity of 5 kN.

Load–deflection (P–δ) diagrams were plotted by controlling the crack mouth opening displacement. The latter was increased at a constant rate of 2.5×10^{-7} m/s.

On the other hand, for higher slenderness values ($\lambda_3, \lambda_4, \lambda_5$) the negative impulse was measured by means of the following set-up (see Fig. 7):

—MTS machine (5 kN max. loading capacity) with constant displacement rate control (5×10^{-4} m/s).

—Impact force transducer, type PCB, Pietronics 200 A03, with a maximum allowable dynamic force of 500 lb (lb = 4.44 N) and a maximum allowable static force of 5000 lb, placed between specimen and loading machine.

The transducer output signal supplied the input for a Fourier analyser. At the same time, from the P–δ branch before failure the elastic energy W_e stored in the specimen was computed (Table 2).

Table 1. Characteristics of the Carrara marble specimens and slenderness values

Type of test	Slenderness $\lambda = l/b$	Support span m·10^{-2}	Sizes and notch depth [m·10^{-2}] b	L	t	a	Density kg/m^3
Static tests	$\lambda_1 = 2.6$	16	6	20	2	0.1	$2.46 \cdot 10^3$
	$\lambda_2 = 4$	16	4	20	2	0.1	$2.46 \cdot 10^3$
	$\lambda_3 = 8$	16	2	20	2	0.1	$2.46 \cdot 10^3$
Dynamic tests	$\lambda_3 = 8$	16	2	20	2	0.1	$2.46 \cdot 10^3$
	$\lambda_4 = 9.5$	19	2	20	4	0.1	$2.46 \cdot 10^3$
	$\lambda_5 = 12$	24	2	30	6	0.1	$2.46 \cdot 10^3$

Table 2. Values of W^* and W^*/W_e measured through static tests and negative impulse method (Carrara marble specimens tested in bending)

Type of test	Static tests			Dynamic tests		
Slenderness $\lambda = l/b$	$\lambda_1 = 2.6$	$\lambda_2 = 4$	$\lambda_3 = 8$	$\lambda_3 = 8$	$\lambda_4 = 9.5$	$\lambda_5 = 12$
$\int F\,dt$ [N·sec]	—	—	—	0.023	0.052	0.083
W^* [N·m·10^{-3}]	13.2	7.5	4.9	4.5	20	28.2
W_e [N·m·10^{-3}]	328.0	183.0	60.9	71.8	150.6	216.1
W^*/W_e	4.03%	4.09%	8.04%	6.26%	13.28%	13.04%

INTERPRETATION AND DISCUSSION OF THE RESULTS

Figure 8 shows the load vs deflection diagrams obtained statically for the less slender specimens (slenderness values $\lambda_1, \lambda_2, \lambda_3$). The W^* energy, represented by the shadowed area, and the elastic energy W_e, i.e. the area under the curve before failure, are given in Table 2.

Figure 9 (a, b, c) shows the force vs time diagrams obtained by means of the dynamic transducer during the failure process of the slenderer specimens (slenderness values $\lambda_3, \lambda_4, \lambda_5$).

The negative impulse $\int F\,dt$ (compression) is represented by the shadowed area. From the impulse (see Table 2), the value of W^* can be determined by means of eqs (16)–(22).

The values of W^* and W_e obtained through dynamic measurements are also given in Table 2. It should be observed that the value of the ratio W^*/W_e given in the last line of the same table tends to increase by increasing specimen slenderness and reaches a value equal to about 13%, which was measured dynamically.

CONCLUSIONS

(1) The failure of Carrara marble specimens tested in bending, with slenderness $\lambda = l/b$ varying between 3 and 12, takes place catastrophically with a remarkable release of energy W^*.

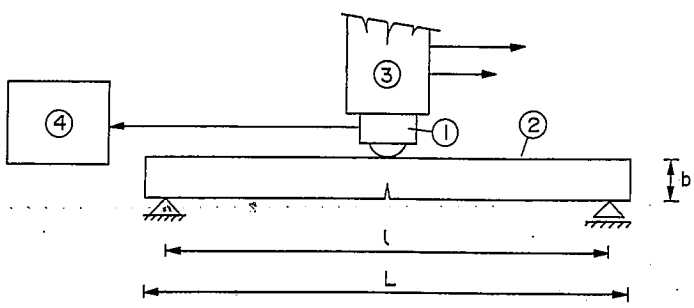

Fig. 7. Testing apparatus: (1) impulse transducer; (2) specimen; (3) MTS machine; (4) Fourier analyser.

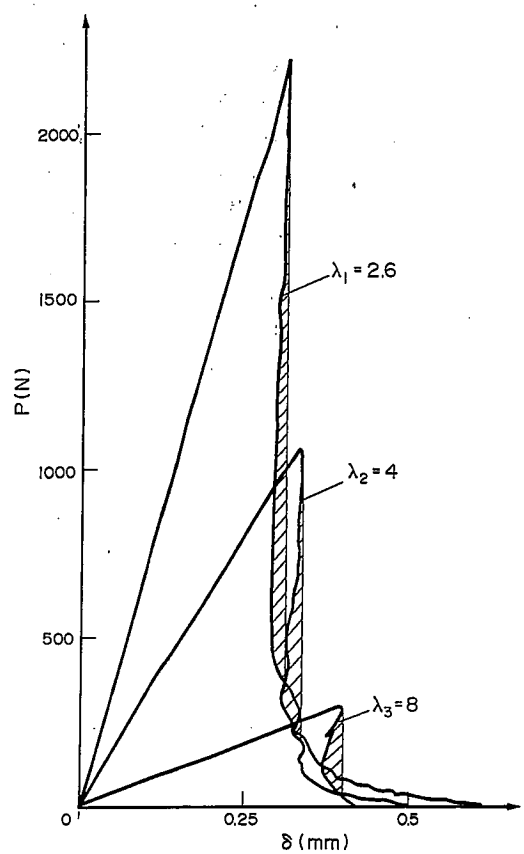

Fig. 8. Experimental load–deflection diagrams obtained statically for low slenderness specimens.

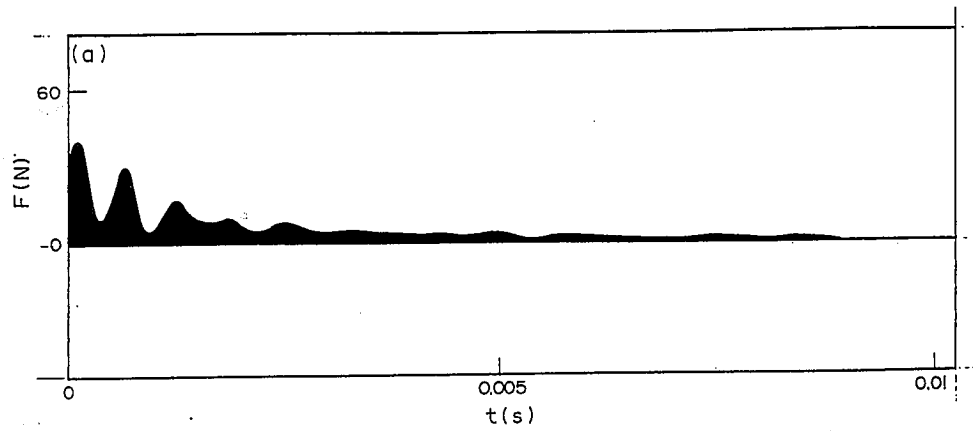

Fig. 9(a). Impulsive force F vs time (slenderness $\lambda_3 = 8$).

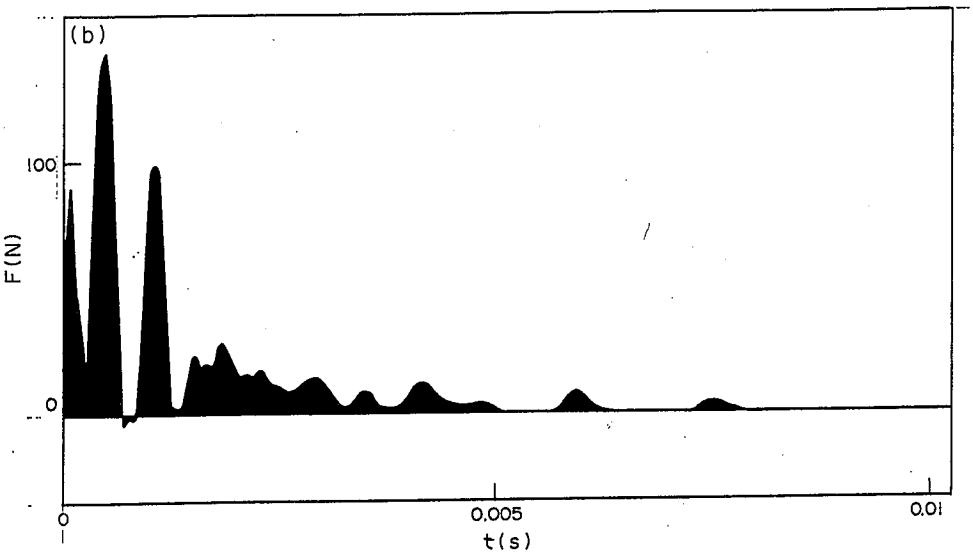

Fig. 9(b). Impulsive force F vs time (slenderness $\lambda_4 = 9.5$).

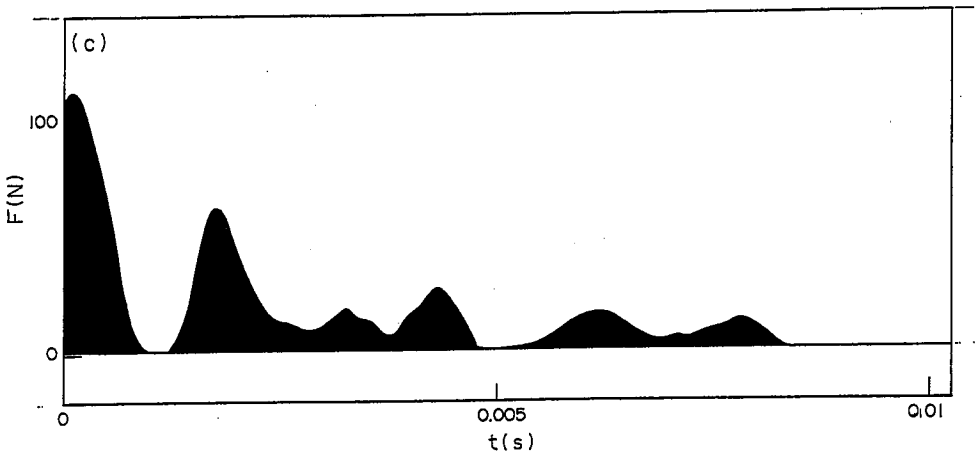

Fig. 9(c). Impulsive force F vs time (slenderness $\lambda_5 = 12$).

(2) The ratio W^*/W_e, i.e. the ratio between the recovered energy and the elastic energy stored at failure, tends to increase by increasing specimen length in agreement with the theoretical prediction of eq. (13).

(3) For the higher slenderness values, failure becomes uncontrollable and instantaneous. In this case the ratio W^*/W_e, measured through the negative impulse, reaches a value of about 13%.

Acknowledgements—The authors wish to thank Mr Vincenzo Di Vasto of the Dipartimento di Ingegneria Strutturale del Politecnico di Torino, for his valuable help in carrying out the experimental tests. The financial support of the Department of Education (M.P.I.) and of the National Research Council (C.N.R.) is also gratefully acknowledged.

REFERENCES

[1] A. Carpinteri, Interpretation of the Griffith instability as a bifurcation of the global equilibrium. N.A.T.O. Advanced Research Workshop on Application of Fracture Mechanics to Cementitious Composites, Northwestern University, 4–7, Sept. 1984 (Edited by S. P. Shah). pp. 287–316 Martinus Nijhoff, The Hague (1985).
[2] A. Carpinteri, Limit analysis for elastic-softening structures: scale and slenderness influence on global brittleness. Euromech Colloquium 204, Structure and Crack Propagation in Brittle Matrix Composite Materials, Jablonna (Poland), November 12–15, 1985 (Edited by A. M. Brandt and I. H. Marshall) Brittle Matrix Composites, Vol. 1, pp. 497–508. Elsevier Applied Science, Amsterdam (1986).
[3] F. Ouchterlony, Fracture toughness testing of rock, *Rock Fracture Mechanics* (Edited by H. P. Rossmanith). Springer, Wien (1983).
[4] P. Bocca, A. Carpinteri and S. Valente, On the applicability of fracture mechanics to masonry. 8th International Brick/Block Masonry Conference, Dublin, Ireland (1988).
[5] L. Biolzi, S. Cangiano, G. Tognon and A. Carpinteri, Snap-back softening instability in high strength concrete beams. SEM-RILEM International Conference on Fracture of Concrete and Rock, Houston, Texas (June 1987). *Mater. Struct.* to appear.
[6] P. Bocca, Evaluation of the released energy during catastrophic failure, to appear.
[7] S. Okubo and Y. Nishimatsu, Uniaxial compression testing using a linear combination of stress and strain as the control variable. *Int. J. Rock Mech. Min. Sci. & Geomech. Abstr.* **22**, 323–330 (1985).
[8] J. A. Hudson, E. T. Brown and C. Fairhurst, Optimizing the control of rock failure in servo-controlled laboratory tests. *Rock Mech.* **3**, 217–224 (1971).

(*Received for publication* 16 *November* 1988)